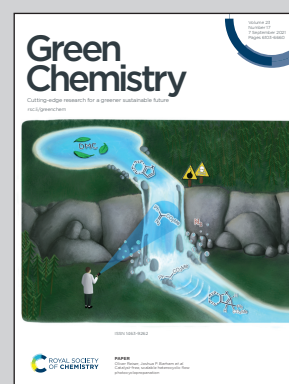


An article presented by Associate Professor Xin Ge and Professor Xuemin Liu *et al.* from Jiangnan University, China and Professor Shaodong Zhou from Zhejiang University, China.

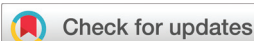
Interfacing sugar-based surfactant micelles and Cu nanoparticles: a nanoreactor for C-S coupling reactions in water

A simple and sustainable synergistic catalytic protocol by interfacing sugar-based surfactant GluM and Cu<sub>2</sub>O nanoparticles was developed for C-S coupling reactions in water. The newly designed sugar-based surfactant GluM was synthesized by the condensation of amine-terminated polyether M2070 with the glucose and the PEG chain was introduced to stabilize the nanoparticles. Cu<sub>2</sub>O nanoparticles were formed by the *in-situ* reduction of copper salt in the aqueous solution of sugar-based surfactant. The interactions between nanomicelles and Cu<sub>2</sub>O NPs to reinforce the micellar effect were revealed.

As featured in:



See Shaodong Zhou, Xuemin Liu *et al.*, *Green Chem.*, 2021, **23**, 6322.

Cite this: *Green Chem.*, 2021, **23**, 6322Received 11th May 2021,  
Accepted 21st July 2021

DOI: 10.1039/d1gc01659h

rsc.li/greenchem

## Interfacing sugar-based surfactant micelles and Cu nanoparticles: a nanoreactor for C–S coupling reactions in water†

Xin Ge,<sup>a,b</sup> Weili Song,<sup>a</sup> Xi He,<sup>a</sup> Jinguo Yang,<sup>a</sup> Chao Qian,<sup>c</sup> Shaodong Zhou<sup>\*c</sup> and Xuemin Liu<sup>\*a</sup>

A simple and sustainable synergistic catalytic protocol by interfacing nanomicelles and metal nanoparticles (MNPs) is reported for C–S coupling reactions in water. The sugar-based surfactant GluM was synthesized by introducing a PEG chain to stabilize MNPs and self-assembled to form nanomicelles. Cu<sub>2</sub>O nanoparticles were generated *via in situ* reduction of copper salt in an aqueous solution of the sugar-based surfactant. The nature of the interaction between nanomicelles and Cu<sub>2</sub>O nanoparticles was revealed by XPS, XRD, *in situ* IR, TEM, and <sup>1</sup>H NMR. A broad substrate scope with moderate to excellent yields was documented and the recycling of the GluM/Cu aqueous mixture was surprising.

### Introduction

Nature has been optimizing various biochemical reactions in water for billions of years.<sup>1</sup> Although water is considered an inexpensive, economical, safe, non-toxic, and sustainable solvent, its use in the chemical and pharmaceutical industries is often limited by the immiscibility of the reactants.<sup>2–4</sup> Therefore, amphiphilic molecule-mediated aqueous–organic reactions employing water as a solvent, such as micellar catalysis<sup>5–9</sup> and vesicular catalysis,<sup>10,11</sup> have been developed by Kobayashi,<sup>12,13</sup> Uozumi,<sup>14</sup> Lipshutz,<sup>15–21</sup> Handa,<sup>22–24</sup> and others.<sup>25–28</sup> The hydrophobic pockets in the self-assembled nanoreactor of amphiphilic molecules hold the oleophilic substrates together to “dissolve” them in water. Particularly, micellar catalysis that involves a nanoreactor for hydrophobic substances is attracting significant attention. Compared with commercially available

surfactants, newly designed surfactants like TPGS-750-M,<sup>29–33</sup> FI-750-M,<sup>21–24,34</sup> and PTS<sup>35–38</sup> are of higher universality and thus suitable for various organic reactions in water. Although enormous achievements in micellar catalysis have been made in recent years, the concept of using metal nanoparticles (MNPs) in micellar catalysis in water is still in its infancy.<sup>39</sup> Recently, MNP-catalyzed Suzuki–Miyaura,<sup>40–42</sup> Sonogashira,<sup>43</sup> Buchwald–Hartwig,<sup>44</sup> Mizoroki–Heck coupling,<sup>45</sup> and reduction reactions<sup>46–48</sup> have been reported to proceed successfully under mild conditions *via* micellar catalysis. Moreover, the “nano-to-nano” effects, where nanomicelles can house and deliver substrates to MNPs, are proposed. Such efficient catalytic activity originates from the synergistic effect between nanomicelles and MNPs: (i) a high concentration of substrates is enriched in nanomicelles, (ii) MNPs (*e.g.* Pd, Cu and Ni) are stabilized by the hydrophilic polyethylene glycol (PEG) chain outside nanomicelles, and (iii) the substrates enriched in nanomicelles are delivered to the metal catalyst. The above phenomenon of needle-like or rod-like MNPs associated with spherical micelles has been observed by cryo-TEM analysis. Despite the high catalytic efficiency of MNP-containing micellar catalysts, the preparation of MNPs is generally complicated.<sup>47,49–53</sup> For example, Pd NPs were obtained by reducing Pd(OAc)<sub>2</sub> with NaBH<sub>4</sub> in aqueous TPGS-750-M at room temperature.<sup>54</sup> Similarly, Fe-based MNPs were prepared through the reduction of FeCl<sub>3</sub>, that either naturally contains Pd or is externally doped with metal salts at the ppm level in the presence of a ligand, with Grignard’s reagent (*e.g.* MeMgCl, MeMgBr) in THF.<sup>45</sup> Nevertheless, it is always challenging and interesting to explore green, sustainable and simple protocols for the preparation of MNPs.

On a different note, C–S coupling catalyzed by transition metals,<sup>55,56</sup> especially Cu,<sup>57–60</sup> continues to attract much attention, as the C–S bond constitutes the functional motif of various biological and pharmaceutical compounds.<sup>61</sup> Furthermore, MNP catalysis in aqueous micelle solution for the formation of the C–S bond is regarded as the next step for sustainable catalysis.<sup>62</sup> In 1995, Suzuki *et al.*<sup>63</sup> reported for the first time the copper-catalyzed coupling of sulfinate

<sup>a</sup>School of Chemical and Material Engineering, Jiangnan University, Wuxi, P.R. China. E-mail: lxm@jiangnan.edu.cn

<sup>b</sup>Key Laboratory of Biomass Chemical Engineering of Ministry of Education, Zhejiang University, Hangzhou, P.R. China

<sup>c</sup>Zhejiang Provincial Key Laboratory of Advanced Chemical Engineering Manufacture Technology, College of Chemical and Biological Engineering, Zhejiang University, Hangzhou, P.R. China. E-mail: szhou@zju.edu.cn

†Electronic supplementary information (ESI) available. See DOI: 10.1039/d1gc01659h

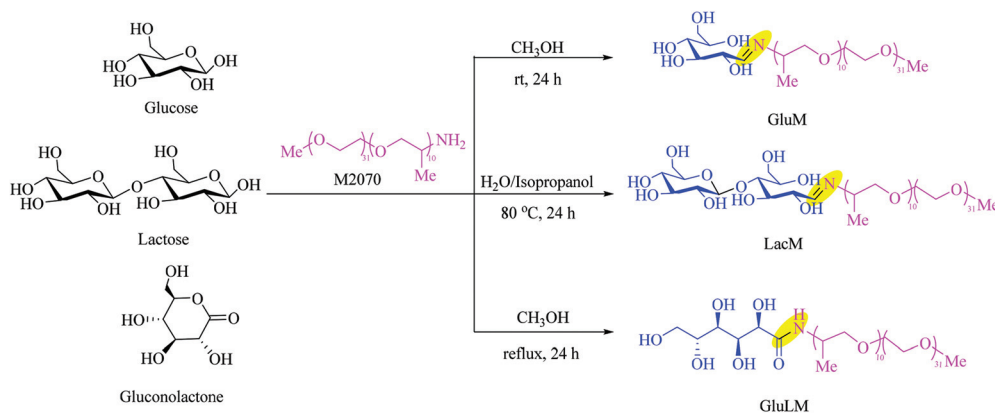
salts with aryl halides to prepare sulfones. Various ligands, such as diamine,<sup>60</sup> proline,<sup>64</sup> 1,10-phenanthroline<sup>65</sup> and D-glucosamine,<sup>66</sup> have been developed. However, these systems still rely on harmful and unrecoverable organic solvents like DMSO and DMF. In 2019, we reported sugar-based surfactants with a glucose or lactose unit as the hydrophilic head; these surfactants were designed as the ligand and micelle constructor for C–S coupling in water.<sup>25</sup> What remained to be explored is the recycling of the copper catalyst as well as the effect of MNPs on catalysis. As green and biodegradable natural compounds, sugars act as reducing and stabilizing agents in the formation of MNPs. For example, sucrose and glucose were used as reducing agents for *in situ* synthesis of Au NPs<sup>67</sup> and Pd NPs,<sup>68</sup> respectively. Sugars are composed of polyhydric hydrophilic structures that produce amphiphilic substances by attaching the hydrophobic chain of sugar-based surfactants.<sup>69</sup> In addition, sugar-based surfactants are eco-friendly, renewable, and biodegradable which play an important role in cosmetics, pharmaceuticals, biochemistry, and gene transfection.<sup>70–74</sup> Moreover, it has remained uncovered whether it is possible to interface sugar-based surfactant micelles and *in situ* generated MNPs as a nanoreactor for organic reactions in water. In this work, a new sugar-based surfactant is designed by introducing a PEG chain to stabilize MNPs. Cu<sub>2</sub>O NPs were synthesized simply by *in situ* reduction of copper salt in an aqueous solution of the sugar-based surfactant. Furthermore, the MNP catalyst can interface with the amphiphilic molecules to inhibit the MNP aggregation and reinforce the micellar effect. We now report on simple, green, and sustainable NP technology for micelle-enabled C–S coupling in water.

## Results and discussion

Considering the stabilization of the PEG chain for MNPs outside the nanomicelles, amine-terminated polyether M2070, a nonionic surfactant based on a copolymer backbone of the PEG chain, was introduced to provide a nanomicelle environment.<sup>75</sup> Combined with the reducing character of sugar, sugar-based

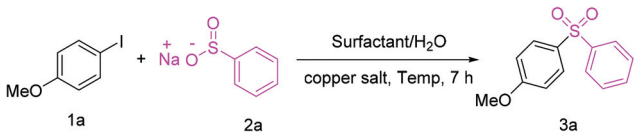
surfactants (GluM, LacM, and GluLM) were prepared by the condensation of the primary amine of M2070 with glucose, lactose, and gluconolactone (in Scheme 1). The critical micelle concentration (CMC) of surfactants is an important parameter, which justifies the formation of micelles. The surface tension ( $\gamma$ ) of these sugar-based surfactants is determined (Fig. S1†) and the CMC values are summarized in Table S1.† It was revealed that the CMC values of three sugar-based surfactants were lower than that of M2070. Thus, the head group has a great influence on the properties of the surfactant.<sup>76,77</sup> Furthermore, it is clear that sugar-based surfactants are successfully synthesized.

Initially, the catalytic performance of these sugar-based non-ionic surfactants was evaluated by the C–S coupling of *p*-iodoanisole with sodium benzenesulfonate as a model reaction. Surfactants such as M2070, GluM, LacM, and GluLM were examined (Table 1, entries 2–4). The catalytic performance of GluM was superior to others and the yield of the desired product was 86%. Moreover, no product was formed in the absence of a surfactant, indicating that the amphiphile was essential for C–S coupling in water (Table 1, entry 1). Subsequently, the experimental conditions were optimized that revealed the dependence of the yield on several parameters, most notably the concentration of the surfactant and the copper source. Thus, the effect of various conditions on the yield of the desired product was investigated. As the concentration of GluM was increased, higher yields were obtained (Table 1, entries 5–8). Further increasing the concentration above 5 mM did not affect the yield. Thus, the importance of the micellar environment on the reaction was justified, and a 5 mM concentration was selected for further investigation. Next, various copper sources, *i.e.*, CuI, CuBr, CuCl, Cu(OAc)<sub>2</sub>, and CuSO<sub>4</sub>, were examined (Table 1, entries 8–12). Although all copper salts initiated the C–S coupling, Cu(OAc)<sub>2</sub> outperformed the others. Subsequently, on screening the loading of copper (Table 1, entries 8 and 13–15), it was found that the optimal loading was 3 mol%, which is lower than those in other similar reports.<sup>25,78</sup> Finally, the effect of different temperatures was probed (Table 1, entries 15–17). The yield increased with the reaction temperature.



**Scheme 1** Synthesis of sugar-based surfactants (GluM, LacM, GluLM).

Table 1 Optimization of the reaction conditions



Entry	Surfactant	Copper salt	Temp./°C	Yield <sup>g</sup> /%
1	—	Cu(OAc) <sub>2</sub>	100	Trace
2	M2070 <sup>a</sup>	Cu(OAc) <sub>2</sub>	100	54
3	LacM <sup>a</sup>	Cu(OAc) <sub>2</sub>	100	62
4	GluLM <sup>a</sup>	Cu(OAc) <sub>2</sub>	100	73
5	GluM <sup>a</sup>	Cu(OAc) <sub>2</sub>	100	86
6	GluM <sup>b</sup>	Cu(OAc) <sub>2</sub>	100	72
7	GluM <sup>c</sup>	Cu(OAc) <sub>2</sub>	100	77
8	GluM	Cu(OAc) <sub>2</sub>	100	87
9	GluM	CuI	100	55
10	GluM	CuBr	100	71
11	GluM	CuCl	100	59
12	GluM	CuSO <sub>4</sub>	100	64
13	GluM	Cu(OAc) <sub>2</sub> <sup>d</sup>	100	43
14	GluM	Cu(OAc) <sub>2</sub> <sup>e</sup>	100	58
15	GluM	Cu(OAc) <sub>2</sub> <sup>f</sup>	100	92
16	GluM	Cu(OAc) <sub>2</sub> <sup>f</sup>	80	21
17	GluM	Cu(OAc) <sub>2</sub> <sup>f</sup>	90	45

Reaction conditions: *p*-iodoanisole (1.0 mmol), sodium benzenesulfinate (1.2 mmol), copper salt (0.1 mmol), and surfactant (0.05 mmol) in 10 mL of water for 7 h. <sup>a</sup>0.1 mmol surfactant. <sup>b</sup>0.005 mmol GluM. <sup>c</sup>0.025 mmol GluM. <sup>d</sup>0.01 mmol Cu(OAc)<sub>2</sub>. <sup>e</sup>0.02 mmol Cu(OAc)<sub>2</sub>. <sup>f</sup>0.03 mmol Cu(OAc)<sub>2</sub>. <sup>g</sup>Isolated yield.

To study the metallic changes in micellar solutions, *in vitro* chelation of surfactants and copper salts was carried out (in Fig. 1a). When surfactants and Cu(OAc)<sub>2</sub> were stirred at 100 °C in water, the color of the mixtures changed. After cooling the mixtures, the solid powder was precipitated and collected. The X-ray diffraction (XRD) patterns of the solid powders are

shown in Fig. 1b. Surprisingly, GluM@Cu and LacM@Cu exhibited reflections at 29.6°, 36.5°, 42.4°, 61.5°, and 73.7° corresponding to the *hkl* planes (110), (111), (200), (220), and (311) of Cu<sub>2</sub>O. Besides, M2070@Cu, exhibited reflections at 32.5°, 35.5°, 38.7°, 48.7°, 53.4°, 58°, 61.5°, and 65.7° corresponding to the *hkl* planes (−110), (002), (111), (−202), (020), (202), (−113) and (022) of CuO (JCPDS file no. 89-2529). However, no reflections were detected in the XRD patterns of GluLM@Cu. Furthermore, XPS analysis was carried out to investigate the surface oxidation states of copper. As shown in Fig. 1c, binding energies for GluM@Cu and LacM@Cu were observed at 932 eV and 952 eV for Cu 2p<sub>3/2</sub> and Cu 2p<sub>1/2</sub>, respectively, and the spin-orbit splitting was 20 eV.<sup>79</sup> For M2070@Cu and GluLM@Cu, the shake-up peaks at 942.8 eV and 963.4 eV were assigned to the Cu<sup>2+</sup> species.<sup>80</sup> In addition, in the Cu 2p spectrum of GluLM@Cu, the peaks at 932.2 eV and 934.3 eV belonged to Cu(I) and Cu(II), respectively.<sup>80</sup> Thus, the XPS results were consistent with the XRD patterns. Finally, UV-vis spectroscopy confirmed the valency of the Cu species. As shown in Fig. S2,† a strong absorption peak was observed at 200–500 nm, consistent with previous reports on Cu<sub>2</sub>O nanostructures.

After reduction of Cu(OAc)<sub>2</sub> to Cu<sub>2</sub>O, the nature of the *in situ* generated Cu<sub>2</sub>O and nanomicelles in the aqueous solution was investigated. Under the same conditions, H<sub>2</sub>O<sup>18</sup> was used as a solvent to prepare Cu<sub>2</sub>O. Additional tests were conducted for the synthesized Cu<sub>2</sub>O. As shown in Fig. S3,† the signal of *m/z* = 18 was detected and the signal of *m/z* = 20 was not observed, indicating that the oxygen of Cu<sub>2</sub>O can only be derived from the copper acetate structure. Besides, Fig. 2a shows that the spherical micelles formed by GluM at 100 °C were averagely 22.46 nm. High-resolution transmission electron microscopy (HRTEM) analysis of the *in situ* generated Cu<sub>2</sub>O in the presence of aqueous GluM revealed a uniform

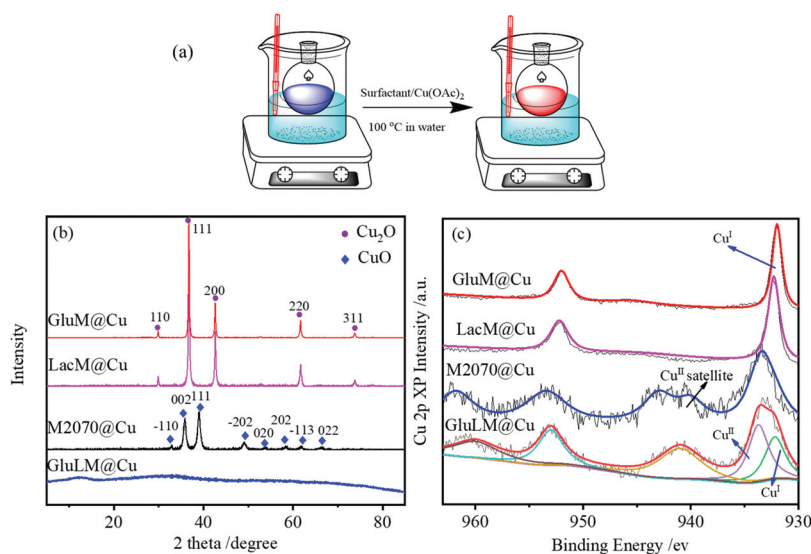


Fig. 1 (a) Schematic representation of mixing of surfactants and Cu(OAc)<sub>2</sub> in water. (b) XRD patterns for GluM@Cu (red), LacM@Cu (pink), M2070@Cu (black) and GluLM@Cu (blue). (c) Cu 2p XPS spectra for GluM@Cu, LacM@Cu, M2070@Cu, and GluLM@Cu from top to bottom.

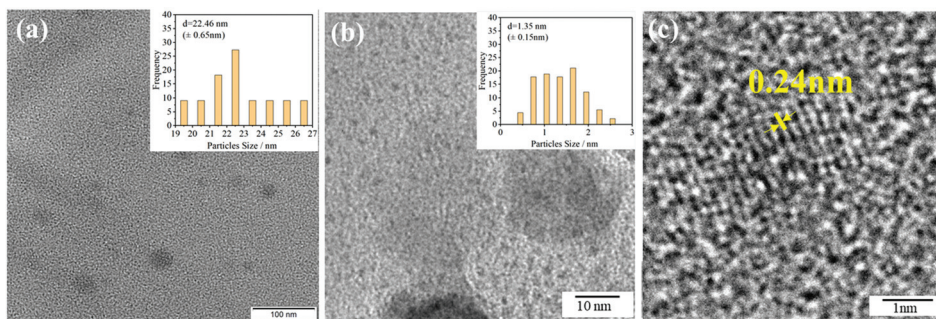


Fig. 2 (a) TEM images of a 5 mM GluM aqueous sample at 100 °C. (b and c) HRTEM images of GluM @Cu in water at 100 °C.

spherical morphology of nanoparticles (in Fig. 2b). The average size of  $\text{Cu}_2\text{O}$  NPs surrounding the nanomicelles of GluM was 1.35 nm. Furthermore, the lattice fringes of 0.24 nm for the (111) planes on the surface of individual particles were also indicative of the formation of  $\text{Cu}_2\text{O}$  (in Fig. 2c). Due to the stabilization of the PEG chain in GluM, the generated nano-sized copper gathered on the outer surface of micelles or inside the micelles through nano-to-nano effects, presumably enhancing the delivery of substrates from the micellar lipophilic cores.

To gain further insight into the interaction between nanomicelles and  $\text{Cu}_2\text{O}$  NPs, we used *in situ* IR to monitor the interactions. As shown in Fig. 3, when adding  $\text{Cu}(\text{OAc})_2$  to GluM aqueous solution at 100 °C, changes in the characteristic absorption peaks at  $1635\text{ cm}^{-1}$  (C=N stretching vibration) and  $1095\text{ cm}^{-1}$  (C–O stretching vibration) were detected. After some time, the C=N absorption peak was split into three peaks; nevertheless, the C–O absorption peak hardly changed. The emergence of new peaks implied that the  $\text{Cu}_2\text{O}$ -micelle interactions occurring around the Schiff base groups of GluM were crucial for highly efficient catalysis.

As shown in Fig. S4,<sup>†</sup> the micellar size was measured by dynamic light scattering (DLS). The spherical nanomicelles

were composed of 5 mM GluM with an average diameter of *ca.* 30 nm. After dissolving iodobenzene in GluM, the size of aggregates increased to *ca.* 50 nm. Next,  $^1\text{H}$  NMR spectra were used to further explore the dissolution of iodobenzene in micelles. As shown in Fig. S5,<sup>†</sup> the chemical shifts of iodobenzene varied from 7.69, 7.33, 7.09 ppm to 7.86, 7.49, and 7.21 ppm, respectively. From the DLS and  $^1\text{H}$  NMR results, the solubility of iodobenzene in the nanomicelles was proven. GluM provided a sufficient nano-space for the encapsulation and aggregation of the substrate. Therefore, a rational mechanism for the sugar-based surfactant micelles enabling the C–S coupling reaction in water is proposed. Initially, iodobenzene was preferentially dissolved in the core of lipophilic micelles. Meanwhile,  $\text{Cu}_2\text{O}$  NPs were synthesized by the *in situ* reduction of copper salt in an aqueous solution of sugar-based surfactants. Moreover, these NPs were assembled on the outer surface or inside the micelles by the PEG chain. Finally, substrates enriched in the micellar lipophilic cores were delivered to NPs, and the coupling product was generated through oxidative addition and reduction elimination.<sup>25</sup>

Upon revealing the mechanism of synergistic catalysis between MNPs and nanomicelles, the scope of Cu-catalyzed C–

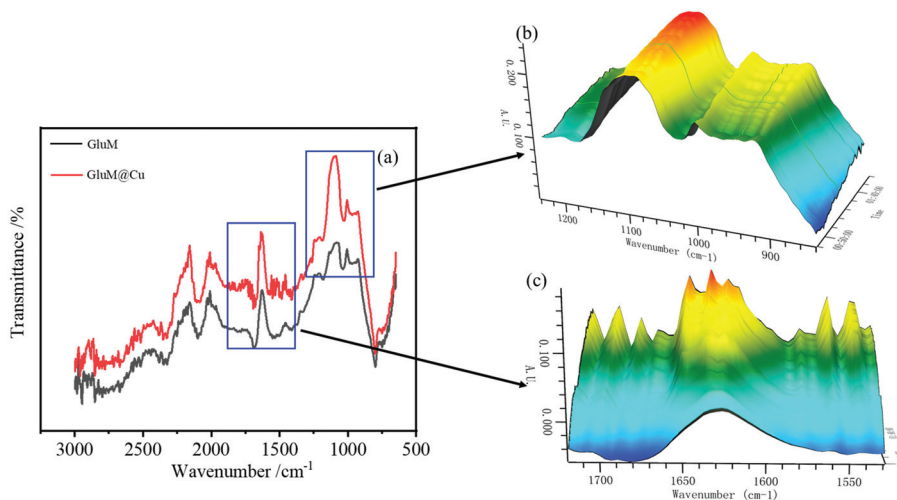


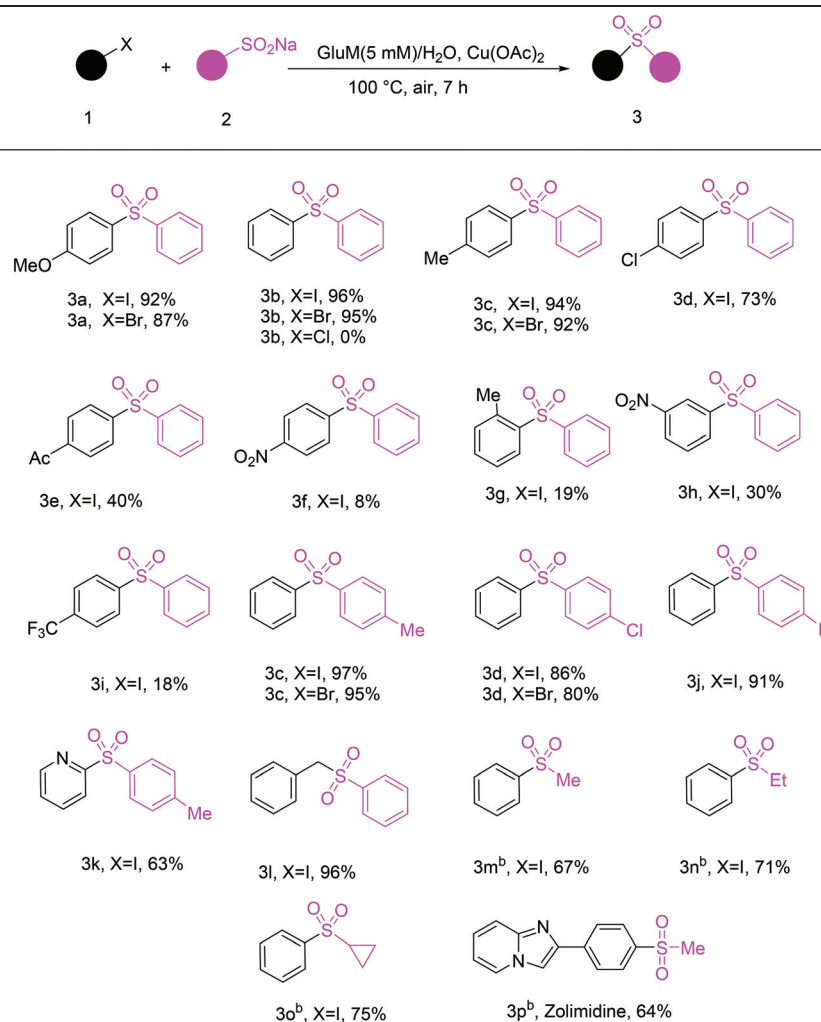
Fig. 3  $\text{Cu}(\text{OAc})_2$  addition to 5 mM GluM aqueous solution at 100 °C. (a) *In situ* ConclRT spectra. (b and c) Overall three-dimensional Fourier transform IR (3D-FTIR) profile.

S coupling in GluM micelles was investigated. As shown in Table 2, an excellent yield of the coupling products was obtained by the reaction of different aryl halides with sodium benzenesulfonate derivatives. The yields of the coupling products from halobenzene with electron-donating groups like 4-OMe (**3a**) and 4-Me (**3c**) were high. By contrast, electron-withdrawing groups, such as 4-Cl (**3d**), 4-Ac (**3e**), 4-NO<sub>2</sub> (**3f**), 3-NO<sub>2</sub> (**3h**), and 4-CF<sub>3</sub> (**3i**), resulted in 18%–73% yields of the coupling products. Besides, *ortho*-methyl substituted iodobenzene gave only 19% yield of the targeted product (**3g**), indicating that space steric hindrance had a crucial effect on the reaction. In addition, good or excellent yields were obtained for benzyl iodide (**3l**) and 2-iodopyridine (**3k**) substrates. Regarding different substituent groups on aryl sulfonates, 4-Me (**3c**), 4-Cl (**3d**), and 4-F (**3j**) substituted substrates resulted in the targeted products with good to excellent yields. In addition, moderate yields of the targeted product were obtained for methyl (**3m**), ethyl (**3n**), and sodium cyclopropylsulfinate (**3o**). Finally,

the application of the protocol for the synthesis of the drug zolimidine from commercially available materials was successful with 64% yield (**3p**).

Finally, the sustainability of the synergistic catalytic system was evaluated. Each cycle of the C–S coupling reactions was carried out under the optimized reaction conditions. As shown in Fig. 4a, once the reaction was completed, the sugar-based surfactant GluM remained in water, while the coupling product was obtained by extraction with ethyl acetate at a constant temperature (50 °C). Fig. 4b shows that the separated GluM/water system still contained the surfactant GluM and Cu<sub>2</sub>O NPs. The size of the GluM micelles was affected by the organic substrate, ranging from 22.46 nm to 48.22 nm. The size of the NPs (1.46 nm) was not so different from that before the reaction, which indicated that a lot of micelles and catalytically active Cu<sub>2</sub>O NPs remained in the aqueous solution after the reaction. Therefore, in the subsequent research of recycling and reuse, only the corresponding substrates were added. As

**Table 2** The substrate scope of Ullmann C–S couplings in an aqueous solution of GluM<sup>a</sup>



<sup>a</sup> Reaction conditions: **1** (1.0 mmol), **2** (1.2 mmol), Cu(OAc)<sub>2</sub> (0.03 mmol) and GluM (0.05 mmol) in water (10 mL) under air at 100 °C for 7 h.

<sup>b</sup> The reaction was carried out at 120 °C.

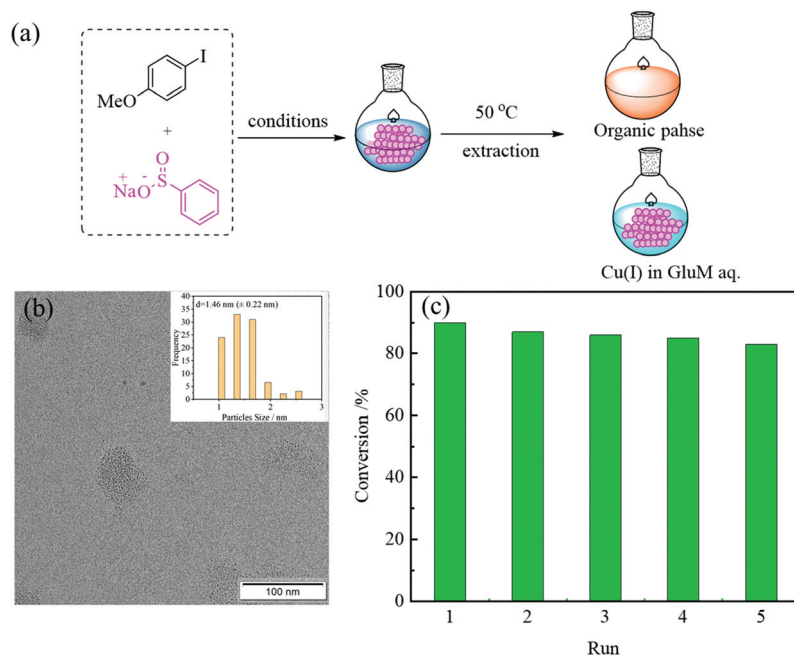


Fig. 4 (a) Hot extraction of GluM micellar catalysis. (b) TEM image of the recycled GluM/water system. (c) Recycling and reuse of GluM/water.

shown in Fig. 4c, it is clear that the separated GluM/water showed good performance after being reused five times. Thus the contamination of wastewater was significantly minimized.

## Conclusions

In summary, a simple and sustainable synergistic catalytic protocol by interfacing a sugar-based surfactant and  $\text{Cu}_2\text{O}$  NPs was developed for C–S coupling reactions in water. The newly designed sugar-based surfactant was synthesized by the condensation of amine-terminated polyether M2070 with glucose and a PEG chain was introduced to stabilize the MNPs.  $\text{Cu}_2\text{O}$  NPs were formed by the *in situ* reduction of copper salt in an aqueous solution of the sugar-based surfactant. The interactions between nanomicelles and  $\text{Cu}_2\text{O}$  NPs to reinforce the micellar effect were revealed by XPS, XRD, *in situ* IR, TEM, and  $^1\text{H}$  NMR. A wide substrate scope with moderate to high yields was documented. The GluM/Cu aqueous mixture was recycled and reused several times.

## Conflicts of interest

There are no conflicts to declare.

## Acknowledgements

The authors are grateful for the financial support from the National Natural Science Foundation of China (22078130, 21878265) and the Fundamental Research Funds for the

Central Universities (2020BCE005). We also appreciate the support for aggregate characterization from the Central Laboratory of School of Chemical and Material Engineering of Jiangnan University.

## References

- 1 A. Acharjee, A. Rakshit, S. Chowdhury and B. Saha, *J. Mol. Liq.*, 2021, **321**, 114897–114899.
- 2 T. Shen, S. Zhou, J. Ruan, X. Chen, X. Liu, X. Ge and C. Qian, *Adv. Colloid Interface Sci.*, 2021, **287**, 102299–102313.
- 3 B. H. Lipshutz, F. Gallou and S. Handa, *ACS Sustainable Chem. Eng.*, 2016, **4**, 5838–5849.
- 4 G. La Sorella, G. Strukul and A. Scarso, *Green Chem.*, 2015, **17**, 644–683.
- 5 A. B. Wood, K. Y. Nandiwale, Y. Mo, B. Jin, A. Pomberger, V. L. Schultz, F. Gallou, K. F. Jensen and B. H. Lipshutz, *Green Chem.*, 2020, **22**, 3441–3444.
- 6 B. H. Lipshutz, T. Y. Yu, H. Pang, Y. Cao and F. Gallou, *Angew. Chem.*, 2020, **60**, 3708–3713.
- 7 B. S. Takale, R. R. Thakore, E. S. Gao, F. Gallou and B. H. Lipshutz, *Green Chem.*, 2020, **22**, 6055–6061.
- 8 B. S. Takale, R. R. Thakore, N. M. Irvine, A. D. Schuitman, X. Li and B. H. Lipshutz, *Org. Lett.*, 2020, **22**, 4823–4827.
- 9 A. B. Wood, M. Cortes-Clerget, J. R. A. Kincaid, B. Akkachairin, V. Singhanian, F. Gallou and B. H. Lipshutz, *Angew. Chem.*, 2020, **59**, 17587–17593.
- 10 G. Hamasaka, T. Muto and Y. Uozumi, *Angew. Chem., Int. Ed.*, 2011, **50**, 4876–4878.

- 11 N. Kaur, S. Kaur, G. Kaur, A. Bhalla, S. Srinivasan and G. R. Chaudhary, *J. Mater. Chem. A*, 2019, **7**, 17306–17314.
- 12 K. Manabe, S. Iimura, X. M. Sun and S. Kobayashi, *J. Am. Chem. Soc.*, 2002, **124**, 11971–11978.
- 13 T. Kitanosono, M. Miyo and S. Kobayashi, *ACS Sustainable Chem. Eng.*, 2016, **4**, 6101–6106.
- 14 G. Hamasaka, T. Muto, Y. Andoh, K. Fujimoto, K. Kato, M. Takata, S. Okazaki and Y. Uozumi, *Chem. – Eur. J.*, 2017, **23**, 1291–1298.
- 15 B. H. Lipshutz, S. Ghorai, A. R. Abela, R. Moser, T. Nishikata, C. Duplais, A. Krasovskiy, R. D. Gaston and R. C. Gadwood, *J. Org. Chem.*, 2011, **76**, 4379–4391.
- 16 B. H. Lipshutz, B. S. Takale, R. R. Thakore, G. Casotti, X. Li and F. Gallou, *Angew. Chem.*, 2020, **60**, 4158–4163.
- 17 N. R. Lee, F. A. Moghadam, F. C. Braga, D. J. Lippincott, B. Zhu, F. Gallou and B. H. Lipshutz, *Org. Lett.*, 2020, **22**, 4949–4954.
- 18 M. Cortes-Clerget, S. E. Spink, G. P. Gallagher, L. Chaisemartin, E. Filaire, J. Y. Berthon and B. H. Lipshutz, *Green Chem.*, 2019, **21**, 2610–2614.
- 19 M.-J. Bu, C. Cai, F. Gallou and B. H. Lipshutz, *Green Chem.*, 2018, **20**, 1233–1237.
- 20 P. Klumphu and B. H. Lipshutz, *J. Org. Chem.*, 2014, **79**, 888–900.
- 21 S. Sharma, N. W. Buchbinder, W. M. Braje and S. Handa, *Org. Lett.*, 2020, **22**, 5737–5740.
- 22 L. Finck, J. Brals, B. Pavuluri, F. Gallou and S. Handa, *J. Org. Chem.*, 2018, **83**, 7366–7372.
- 23 J. D. Smith, T. N. Ansari, M. P. Andersson, D. Yadagiri, F. Ibrahim, S. Liang, G. B. Hammond, F. Gallou and S. Handa, *Green Chem.*, 2018, **20**, 1784–1790.
- 24 J. Brals, J. D. Smith, F. Ibrahim, F. Gallou and S. Handa, *ACS Catal.*, 2017, **7**, 7245–7250.
- 25 X. Ge, S. Zhang, X. Chen, X. Liu and C. Qian, *Green Chem.*, 2019, **21**, 2771–2776.
- 26 A. Donner, K. Hagedorn, L. Mattes, M. Drechsler and S. Polarz, *Chem. – Eur. J.*, 2017, **23**, 18129–18133.
- 27 R. Lambert, A.-L. Wirocius, J. Vignolle and D. Taton, *Polym. Chem.*, 2019, **10**, 460–466.
- 28 F. P. Ballistreri, C. M. A. Gangemi, A. Pappalardo, G. A. Tomaselli, R. M. Toscano and G. T. Sfrazzetto, *Int. J. Mol. Sci.*, 2016, **17**, 1112.
- 29 B. H. Lipshutz, *Curr. Opin. Green. Sust.*, 2018, **11**, 1–8.
- 30 D. J. Lippincott, P. J. Trejo-Soto, F. Gallou and B. H. Lipshutz, *Org. Lett.*, 2018, **20**, 5094–5097.
- 31 N. A. Isley, F. Gallou and B. H. Lipshutz, *J. Am. Chem. Soc.*, 2013, **135**, 17707–17710.
- 32 S. M. Kelly and B. H. Lipshutz, *Org. Lett.*, 2014, **16**, 98–101.
- 33 N. A. Isley, M. S. Hageman and B. H. Lipshutz, *Green Chem.*, 2015, **17**, 893–897.
- 34 S. Handa, F. Ibrahim, T. N. Ansari and F. Gallou, *ChemCatChem*, 2018, **10**, 4229–4233.
- 35 J. C. Fennewald, E. B. Landstrom and B. H. Lipshutz, *Tetrahedron Lett.*, 2015, **56**, 3608–3611.
- 36 M. H. Daniels, J. R. Armand and K. L. Tan, *Org. Lett.*, 2016, **18**, 3310–3313.
- 37 S. Handa, M. P. Andersson, F. Gallou, J. Reilly and B. H. Lipshutz, *Angew. Chem., Int. Ed.*, 2016, **55**, 4914–4918.
- 38 J. S. da Costa, R. K. Braun, P. A. Horn, D. S. Lüdtkke and A. V. Moro, *RSC Adv.*, 2016, **6**, 59935–59938.
- 39 B. H. Lipshutz, *Johnson Matthey Technol. Rev.*, 2017, **61**, 196–202.
- 40 B. S. Takale, R. R. Thakore, S. Handa, F. Gallou, J. Reilly and B. H. Lipshutz, *Chem. Sci.*, 2019, **10**, 8825–8831.
- 41 S. Handa, Y. Wang, F. Gallou and B. H. Lipshutz, *Science*, 2015, **349**, 1087–1091.
- 42 S. Handa, E. D. Slack and B. H. Lipshutz, *Angew. Chem., Int. Ed.*, 2015, **54**, 11994–11998.
- 43 S. Handa, B. Jin, P. P. Bora, Y. Wang, X. Zhang, F. Gallou, J. Reilly and B. H. Lipshutz, *ACS Catal.*, 2019, **9**, 2423–2431.
- 44 T. N. Ansari, A. Taussat, A. H. Clark, M. Nachtegaal, S. Plummer, F. Gallou and S. Handa, *ACS Catal.*, 2019, **9**, 10389–10397.
- 45 H. Pang, Y. Hu, J. Yu, F. Gallou and B. H. Lipshutz, *J. Am. Chem. Soc.*, 2021, **143**, 3373–3382.
- 46 H. Pang, F. Gallou, H. Sohn, J. Camacho-Bunquin, M. Delferro and B. H. Lipshutz, *Green Chem.*, 2018, **20**, 130–135.
- 47 C. M. Gabriel, M. Parmentier, C. Riegert, M. Lanz, S. Handa, B. H. Lipshutz and F. Gallou, *Org. Process Res. Dev.*, 2017, **21**, 247–252.
- 48 J. Feng, S. Handa, F. Gallou and B. H. Lipshutz, *Angew. Chem., Int. Ed.*, 2016, **55**, 8979–8983.
- 49 J. Feng, S. Handa, F. Gallou and P. Bruce, *Angew. Chem.*, 2016, **128**, 9125–9129.
- 50 S. Handa, J. D. Smith, M. S. Hageman, M. Gonzalez and B. H. Lipshutz, *ACS Catal.*, 2016, **6**, 8179–8183.
- 51 A. Adenot, E. B. Landstrom, F. Gallou and B. H. Lipshutz, *Green Chem.*, 2017, **19**, 2506–2509.
- 52 H. Pang, F. Gallou, H. Sohn, J. Camacho-Bunquin, M. Delferro and B. H. Lipshutz, *Green Chem.*, 2018, **20**, 130–135.
- 53 H. Pang, Y. Wang, F. Gallou and B. H. Lipshutz, *J. Am. Chem. Soc.*, 2019, **141**, 17117–17124.
- 54 E. D. Slack, C. M. Gabriel and B. H. Lipshutz, *Angew. Chem., Int. Ed.*, 2014, **53**, 14051–14054.
- 55 I. P. Beletskaya and V. P. Ananikov, *Chem. Rev.*, 2011, **111**, 1596–1636.
- 56 C. F. Lee, Y. C. Liu and S. S. Badsara, *Chem. – Asian J.*, 2014, **9**, 706–722.
- 57 M. E. Shabestari, O. Martin, D. Diaz-Garcia, S. Gomez-Ruiz, V. J. Gonzalez and J. Baselga, *Carbon*, 2020, **161**, 7–16.
- 58 P. Bhanja, S. K. Das, A. K. Patra and A. Bhaumik, *RSC Adv.*, 2016, **6**, 72055–72068.
- 59 J. Mondal, A. Modak, A. Dutta, S. Basu, S. N. Jha, D. Bhattacharyya and A. Bhaumik, *Chem. Commun.*, 2012, **48**, 8000–8002.
- 60 J. M. Baskin and Z. Y. Wang, *Org. Lett.*, 2002, **4**, 4423–4425.
- 61 C. Shen, P. F. Zhang, Q. Sun, S. Q. Bai, T. S. A. Hor and X. G. Liu, *Chem. Soc. Rev.*, 2015, **44**, 291–314.
- 62 M. Cortes-Clerget, J. L. Yu, J. R. A. Kincaid, P. Walde, F. Gallou and B. H. Lipshutz, *Chem. Sci.*, 2021, **12**, 4237–4266.

- 63 H. Suzuki and H. Abe, *Tetrahedron Lett.*, 1995, **36**, 6239–6242.
- 64 W. Zhu and D. W. Ma, *J. Org. Chem.*, 2005, **70**, 2696–2700.
- 65 B. T. V. Srinivas, V. S. Rawat, K. Konda and B. Sreedhar, *Adv. Synth. Catal.*, 2014, **356**, 805–817.
- 66 M. Yang, H. Y. Shen, Y. Y. Li, C. Shen and P. F. Zhang, *RSC Adv.*, 2014, **4**, 26295–26300.
- 67 H. Yokota, M. Kadowaki, T. Matsuura, H. Imanaka, N. Ishida and K. Imamura, *Langmuir*, 2020, **36**, 6698–6705.
- 68 A. Monopoli, V. Calo, F. Ciminale, P. Cotugno, C. Angelici, N. Cioffi and A. Nacci, *J. Org. Chem.*, 2010, **75**, 3908–3911.
- 69 N. Drillaud, E. Banaszak-Leonard, I. Pezron and C. Len, *J. Org. Chem.*, 2012, **77**, 9553–9561.
- 70 U. Komorek and K. A. Wilk, *J. Colloid Interface Sci.*, 2004, **271**, 206–211.
- 71 M. J. L. Castro, A. F. Cirelli and J. Kovensky, *J. Surfactants Deterg.*, 2006, **9**, 279–286.
- 72 K. A. Wilk, L. Syper, B. Burczyk, I. Maliszewska, M. Jon and B. W. Domagalska, *J. Surfactants Deterg.*, 2001, **4**, 155–161.
- 73 F. M. Menger and B. N. A. Mbadugha, *J. Am. Chem. Soc.*, 2001, **123**, 875–885.
- 74 K. A. Wilk, L. Syper, B. Burczyk, A. Sokolowski and B. W. Domagalska, *J. Surfactants Deterg.*, 2000, **3**, 185–192.
- 75 X. Ge, W. Song, X. Chen, C. Qian and X. Liu, *Colloids Surf., A*, 2021, **616**, 126263–126274.
- 76 X. M. Liu, X. Liao, S. H. Zhang, S. Chang, L. Cheng, M. Ge and X. Ge, *J. Chem. Eng. Data*, 2019, **64**, 60–68.
- 77 K. Nyuta, T. Yoshimura, K. Tsuchiya, T. Ohkubo, H. Sakai, M. Abe and K. Esumi, *Langmuir*, 2006, **22**, 9187–9191.
- 78 C. Shen, J. Xu, W. Yu and P. Zhang, *Green Chem.*, 2014, **16**, 3007–3012.
- 79 K. Sekar, C. Chuaicham, U. Balijapalli, W. Li, K. Wilson, A. F. Lee and K. Sasaki, *Appl. Catal., B*, 2021, **284**, 119741.
- 80 H. Li, J. Qin, Y. Zhang, S. Xu, J. Du and J. Tang, *RSC Adv.*, 2018, **8**, 39352–39361.